Am J Physiol Heart Circ Physiol 292: H2817–H2823, 2007.
First published February 2, 2007; doi:10.1152/ajpheart.00936.2006.

Wave intensity analysis of left ventricular filling: application of windkessel theory

Jacqueline A. Flewitt, Tracy N. Hobson, Jiun Jr Wang, Clifton R. Johnston, Nigel G. Shrive, Israel Belenkie, Kim H. Parker, and John V. Tyberg

Libin Cardiovascular Institute of Alberta and Departments of Cardiac Sciences, Physiology and Biophysics, Civil Engineering, and Mechanical Engineering, University of Calgary, Calgary, Alberta, Canada

Submitted 29 August 2006; accepted in final form 30 January 2007

Flewitt JA, Hobson TN, Wang JJ, Johnston CR, Shrive NG, Belenkie I, Parker KH, Tyberg JV. Wave intensity analysis of left ventricular filling: application of windkessel theory. *Am J Physiol Heart Circ Physiol* 292: H2817–H2823, 2007. First published February 2, 2007; doi:10.1152/ajpheart.00936.2006.—We extend our recently published windkessel-wave interpretation of vascular function to the wave intensity analysis (WIA) of left ventricular (LV) filling dynamics by separating the pressure changes due to the windkessel from those due to traveling waves. With the use of LV compliance, the change in pressure due solely to LV volume changes (windkessel pressure) can be isolated. Inasmuch as the pressure measured in the cardiovascular system is the sum of its windkessel and wave components (excess pressure), it can be substituted into WIA, yielding the isolated wave effects on LV filling. Our study of six open-chest dogs demonstrated that once the windkessel effects are removed from WIA, the energy of diastolic suction is 2.6 times greater than we previously calculated. Volume-related changes in pressure (i.e., the windkessel or reservoir effect) must be considered first when wave motion is analyzed.

transmitral flow; mitral velocity; E wave; diastolic suction

THE LEFT ATRIUM (LA) was first described as a combined conduit and reservoir by Grant et al. (6). Recently, we adapted the concepts of Otto Frank (4) to describe the large systemic arteries (21) and veins (20) as windkessel-wave systems. The essence of this concept is that the pressure changes that result from changes in volume (i.e., windkessel or reservoir effects) must be assessed and subtracted from the measured changes in pressure before wave motion can be evaluated appropriately. Here, we extend that approach to an analysis of transmitral flow dynamics and left ventricular (LV) filling. Because the left heart is a reservoir and functions similar to a windkessel, any change in its volume will be accompanied by a change in pressure; the reservoir pressure, which is related to volume changes through compliance (21), should be subtracted from the measured pressure (P_{meas}) to reveal the "excess" pressure (P_{ex}) (10) that is caused solely by waves.

Wave intensity analysis (WIA) uses changes in pressure and velocity to quantify wave energy. However, the measured change in pressure may not be due entirely to waves; if we consider the reservoir function of the left heart, it becomes apparent that there needs to be a correction for the effects of compliance. As a first approximation of left heart compliance, we have used a linear estimation of the compliance of the passive LV to separate out the change in pressure caused by waves from that due to LV compliance (C_{LV}). Only the change in pressure caused by waves should be incorporated into transmitral WIA.

Glossary

A	Area (cm^2)
A_d	Area at zero-pressure intercept (cm^2)
BCW	Backward-going compression wave
BEW	Backward-going expansion wave
c	Wave speed (m/s)
C	Compliance (cm^3/mmHg)
D	Distensibility ($mmHg^{-1}$)
D_{ap}	LV anterior-posterior dimension (mm)
D_{ba}	LV base-apex dimension (mm)
D_{sfw}	LV septum-free wall dimension (mm)
DS	Diastolic suction
dI_W	Net intensity (W/m^2)
dI_{W+}	Intensity of forward-going wave (W/m^2)
dI_{W-}	Intensity of backward-going wave (W/m^2)
dP	Incremental change in pressure (mmHg)
dU	Incremental change in velocity (m/s)
FCW	Forward-going compression wave
FEW	Forward-going expansion wave
$I_{W\text{-}DS}$	Energy of early diastolic backward-going wave (i.e., diastolic suction)
K	Volume scaling factor
LA	Left atrium (atrial)
LV	Left ventricle (ventricular)
LVEDP	End-diastolic LV pressure (mmHg)
ρ	Density (kg/m^3)
P	Pressure (mmHg)
P-V	Pressure-volume (i.e., LV pressure-volume loop)
P_{ex}	Excess pressure (mmHg)
P_{meas}	Measured pressure (mmHg)
P_{Wk}	Windkessel pressure (mmHg)
PV	Pulmonary vein(s)
Q	Flow (ml/s)
U	Velocity (m/s)
V	Volume (ml or m^3)
WIA	Wave intensity analysis
Wk	Windkessel

Address for reprint requests and other correspondence: J. V. Tyberg, Health Sciences Centre, Univ. of Calgary, 3330 Hospital Dr. NW, Calgary, AB, T2N 4N1 Canada (e-mail: jtyberg@ucalgary.ca).

The costs of publication of this article were defrayed in part by the payment of page charges. The article must therefore be hereby marked "*advertisement*" in accordance with 18 U.S.C. Section 1734 solely to indicate this fact.

METHODS

Theory

WIA applied to LV filling dynamics. The fundamental principles of WIA are outlined in the APPENDIX. WIA was applied at the mitral valve to quantify the energy of waves traveling to/from the LV throughout diastole. Pressure and velocity were measured at the mitral valve.

LV wave speed (c), which varies considerably throughout the cardiac cycle with changes in LV elastance, can be calculated continuously as

$$c = \sqrt{(1/\rho D)} \quad (1)$$

where ρ is the density of the blood and D is the distensibility of the LV

$$D = (A - A_d)/(P \cdot A) \quad (2)$$

where P is LV pressure, A is LV area, and A_d is area at the zero-pressure intercept (22).

Windkessel. Any compliant structure in the cardiovascular system will behave as a reservoir. Wang et al. developed the windkessel theory in which the arterial (21) and venous (20) systems have been modeled as a blood-conducting system and a reservoir. The reservoir, or windkessel, is a hydraulic integrator where the change in pressure is related to the change in volume via the compliance of the chamber. In the case where we assume compliance to be constant, reservoir pressure is referred to as windkessel pressure (P_{Wk}) to be consistent with previous work (20, 21). P_{meas} has been shown to be the instantaneous summation of a time-varying reservoir (i.e., windkessel) pressure and P_{ex}, which represents the effects of traveling waves (21).

As described above, wave intensity is calculated from incremental changes in pressure. Conventionally, this has been calculated as the change in P_{meas}. On the basis of windkessel theory, P_{meas} should be divided into its reservoir (P_{Wk}) and wave components (P_{ex})

$$dP_{meas} = dP_{ex} + dP_{Wk} \quad (3)$$

Consequently, in this study, wave intensity was calculated from P_{ex}, the change in pressure due solely to waves, thus excluding the effects of compliance.

With the use of linear regression, C_{LV} was estimated as the slope of the LV pressure-volume (P-V) relation (calculated by sonomicrometry) during the interval between the nadir in LV pressure (P_{LV}, when wave action related to early diastolic filling has ceased) and the onset of LA contraction (Fig. 1) (11)

$$C_{LV} = \Delta V_{LV}/\Delta P_{LV} \quad (4)$$

dP_{Wk}, the change in pressure due to the change in volume, was calculated from dV_{LV}, divided by the compliance of the passive LV (C_{LV})

$$dP_{Wk} = dV_{LV}/C_{LV} \quad (5)$$

This correction for dP_{Wk} was applied from the beginning of diastole to the start of LA contraction (Fig. 2*B*). Note that $dP_{ex} = dP_{meas} - dP_{Wk}$.

Correcting WIA for the windkessel. On the basis of *Eq. 3*, the WIA equations (see APPENDIX) can be written in terms of dP_{ex}

$$dI_{W+} = (+\frac{1}{4}\rho c)(dP_{ex} + \rho c dU)^2 \quad (6)$$

$$dI_{W-} = (-\frac{1}{4}\rho c)(dP_{ex} - \rho c dU)^2 \quad (7)$$

$$dP_{+} = \frac{1}{2}(dP_{ex} + \rho c dU) \quad (8)$$

$$dP_{-} = \frac{1}{2}(dP_{ex} - \rho c dU) \quad (9)$$

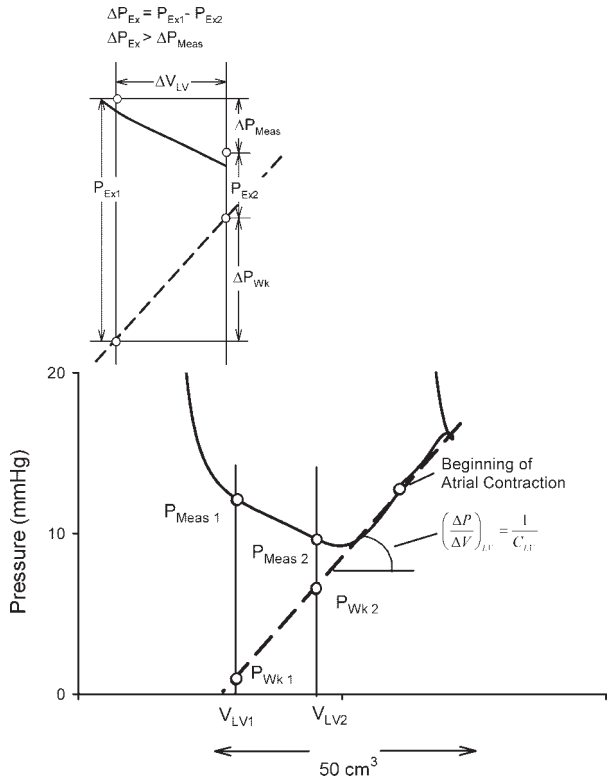

Fig. 1. Correction for passive left ventricular (LV) compliance (C_{LV}, i.e., windkessel effect). As the LV filled incrementally from V_{LV1} to V_{LV2} (where V_{LV} is LV volume), LV pressure decreased from P_{meas1} to P_{meas2} (where P_{meas} is measured pressure). Passive C_{LV} was estimated by fitting a (dashed) line to the LV pressure-volume (P-V) data between the nadir in pressure and the beginning of left atrial (LA) contraction. By extrapolation, this indicates that pressure would have increased from P_{Wk1} to P_{Wk2} (where P_{Wk} is windkessel pressure) simply as the result of incremental filling (ΔV_{LV}). Because $P_{meas} = P_{Wk} + P_{ex}$, this incremental filling was associated with a decrease in wave-related pressure from P_{ex1} to P_{ex2} (where Pex is excess pressure). Incremental change in P_{ex} (ΔP_{ex}) is greater than the incremental change in P_{meas} (ΔP_{meas}).

Experimental Preparation and Protocol

The protocol for the animal experiments conformed to the "Guiding Principles of Research Involving Animals and Human Beings" of the American Physiological Society and was approved by the University of Calgary Animal Care Committee.

Studies were performed in six healthy mongrel dogs (21–27 kg body wt), which were anesthetized initially with thiopental sodium (25 mg/kg); a surgical plane of anesthesia was maintained with fentanyl citrate (4 mg/h iv), adjusted as necessary. The dogs were ventilated with 1:1 nitrous oxide-oxygen via a constant-volume respirator set to deliver a tidal volume of 19 ml/kg at a rate of 18 breaths/min. Blood gases were monitored and ventilatory rates were adjusted to maintain normal levels and pH. Normal body temperature was maintained with a heating pad.

Instrumentation was performed through a midline thoracotomy. Ultrasonic flow probes (Transonic Systems, Ithaca, NY) were placed around the aorta (as close to the aortic valve as possible) and a branch of a pulmonary vein (PV). Micromanometer-tipped catheters (8-Fr, model PC-480, Millar Instruments, Houston, TX) with fluid-filled reference lumens were introduced retrogradely through the femoral artery and the left carotid artery and used to measure pressure in the aorta and the LV, respectively. The tip of the LV catheter was placed close to the mitral valve. Micromanometer-tipped catheters (3.5-Fr, model SPR-524, Millar Instruments) were introduced directly through the appendage and a PV

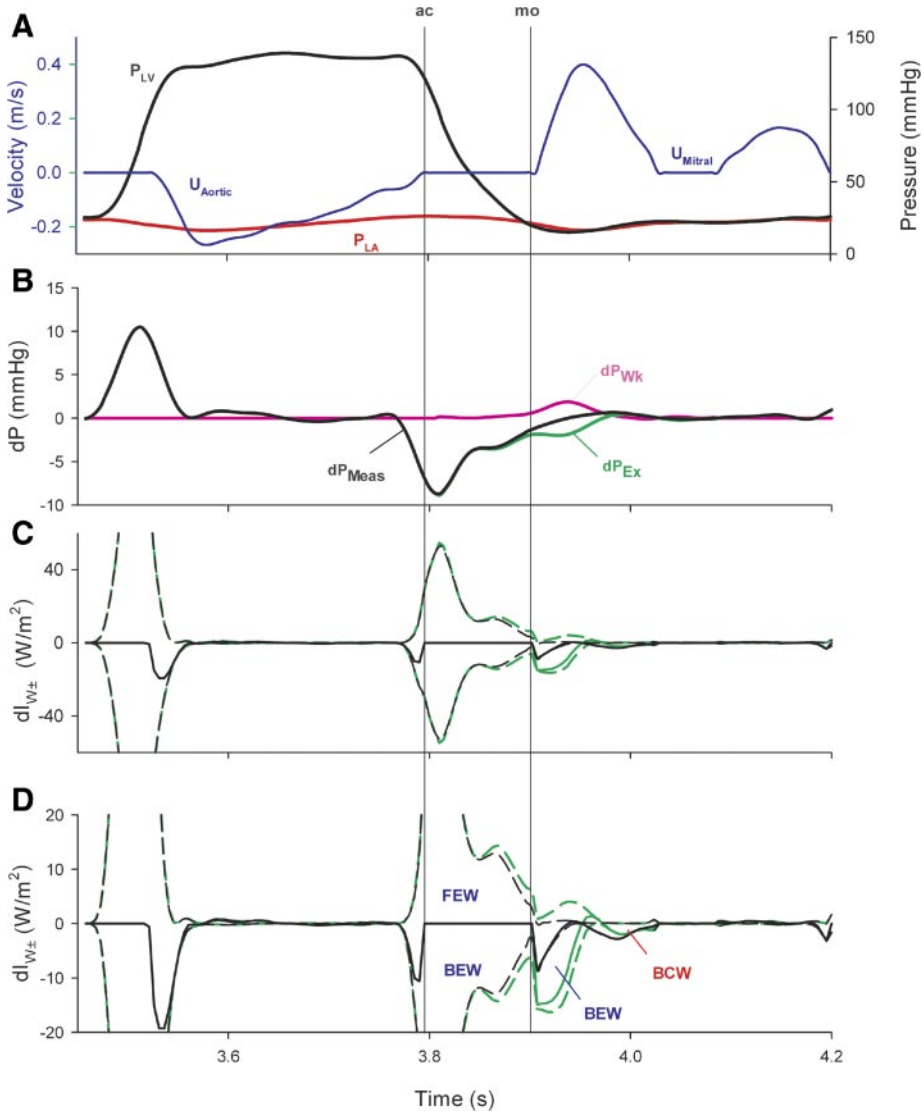

Fig. 2. *A*: hemodynamic recordings from a representative experiment. Black trace, LV pressure (P_{LV}); red trace, LA pressure (P_{LA}); blue traces, mitral velocity (U_{mitral}, measured by Doppler echocardiography) and aortic velocity (U_{aortic}, calculated from aortic flow and scaled so that volume ejected during systole equals volume filled during diastole). By convention, LV filling is represented as positive and emptying as negative. *B*: incremental changes in pressure. Black trace, change in P_{meas} (dP_{meas}); pink trace, change in P_{Wk} (dP_{Wk}); green trace, change in P_{ex} (dP_{ex}). *C*: wave intensity analysis (WIA) results. *D*: WIA results on an expanded scale. Dashed lines, intensities of forward-going (positive) and backward-going (negative) waves [forward-going expansion wave (FEW) and backward-going expansion and compression waves (BEW and BCW, respectively)]; solid lines, net intensity. Black trace, original WIA; dark green trace, corrected WIA. Vertical lines represent aortic valve closure and mitral valve opening.

and used to measure pressure in the PV and LA, respectively. A stiff plastic introducer was used to insert the PV catheter into a right PV. The PV catheter was then advanced to a left PV, different from the PV with the flow transducer. Orthogonal LV dimensions were measured with pairs of sonomicrometry crystals positioned near the endocardium: base-apex (D_{ba}), septum-free wall (D_{sfw}), and anterior-posterior (D_{ap}) dimensions. A large-bore catheter was inserted into the left jugular vein for volume loading. A single-lead ECG was recorded.

After instrumentation, the pericardium was reapproximated with single interrupted sutures (17). The dog was turned slightly toward its right, and a 5-MHz transesophageal probe (model 77020AC, Hewlett-Packard, Palo Alto, CA) was advanced to the level of the heart. The echocardiographic two-chamber, long-axis view(s) was used to place the sample volume at the level of the tips of mitral valve leaflets, and the transducer position was adjusted to record maximum mitral flow velocity (model 5500, Philips Medical Systems, Markham, ON, Canada). The traces were recorded on VHS videotape for subsequent analysis. Heart rate was maintained at 60–90 beats/min with ULFS-49 (7) as needed. The ventilator was turned off at end expiration during each 30-s period of data collection.

Data were first recorded under control conditions at an LV end-diastolic pressure (LVEDP) of ~7 mmHg. By volume loading (10% pentastarch in 0.9% NaCl; Pentaspan, Bristol-Myers Squibb Canada), LVEDP was increased in ~3-mmHg increments to ~25 mmHg; data were recorded at each level.

Data Handling

Signals were recorded at a sampling rate of ~200 Hz using data acquisition software (CARDIOSOFT, Sonometrics, London, ON, Canada). A frame counter was used to synchronize the hemodynamic data and Doppler flow velocities. Static images of Doppler flow velocity at the mitral valve and the ECG were captured from videotape (Video Studio 6, Ulead Systems, Taipei, Taiwan) and digitized using a custom-made program (Matlab, Mathworks, Natick, MA); the ECG and mitral flow velocity waveforms were exported to a spreadsheet (Excel, Microsoft Office, Microsoft, Redmond, WA). Sonomicrometry dimension recordings were "cleansed" (CARDIOSOFT) of extraneous noise. All hemodynamic data were exported to a data-analysis program (CVWorks, Advanced Measurements, Calgary, AB, Canada), and the data from the beat selected for analysis were isolated. The frame count and end-systolic and end-diastolic points were identified. Data were exported to a spreadsheet (Excel) and aligned in time with respect to mitral flow velocity. All data were filtered at 30 Hz (low-pass Butterworth filter; Matlab).

Table 1. *Hemodynamic results under control conditions*

Expt	HR, beats/min	CO, l/min	P_{AO}, mmHg	EDP, mmHg	
				LV	LA
A	65	2.1	89.1	6.2	5.8
B	41	1.4	87.8	7.1	6.4
C	58	2.7	87.3	6.8	6.8
D	49	1.1	69.1	6.5	7.2
E	73	1.4	95.1	4.2	3.8
F	75	2.1	78.0	5.7	5.3
Mean (SD)	60 (12)	1.8 (0.5)	84.4 (8.5)	6.1 (0.9)	5.9 (1.1)

HR, heart rate; CO, cardiac output (stroke volume × HR); $\bar{P}_{ao}$, mean aortic pressure over 1 cardiac cycle; EDP, end-diastolic pressure; LV, left ventricle; LA, left atrium.

LV volume (V_{LV}) was calculated as

$$V_{LV} = K \cdot D_{ba} \cdot D_{sfw} \cdot D_{ap} \quad (10)$$

where *K,* a geometric shape factor (5, 15), was calculated by assuming that the change in V_{LV} during ejection was equal to the stroke volume

$$\Delta V_{LV} = \left(\int Q_{ao} \cdot dt \right) \Big| K \quad (11)$$

where Q_{ao} is aortic flow and *K* was recalculated for each new data set (i.e., after each volume infusion or other manipulation).

RESULTS

Control hemodynamic data are listed in Table 1.

Pooled data for C_{LV} at increasing LVEDPs are displayed in Fig. 3. Exponential decay regression parameters for data from individual experiments are given in Table 2.

WIA

Data from a representative cardiac cycle and the results of WIA are shown in Fig. 2. From end systole to the start of LA contraction, the change in pressure associated with the increasing volume (dP_{Wk}) was calculated and subtracted from the change in P_{meas} (dP_{meas}); the result is the change in pressure due only to wave action (dP_{ex}; Fig. 2*B*). During early diastole, $dP_{Wk} > 0$, increasing the absolute magnitude of dP_{ex}. As the LV relaxes, a backward expansion wave (BEW) slows thecolumn of ejected blood, contributing to aortic valve closure (Fig. 2, *C* and *D*). After valve closure, net intensity becomes zero, because the incremental change in velocity (d*U*) is zero. During isovolumic relaxation, pressure decreases rapidly, due to decreasing elastance. Because of the dP dependence of *Eqs. 6* and *7*, WIA yields equal and opposite intensities. Because LV relaxation is not complete when the mitral valve opens, a net BEW in the LV tends to pull blood from the LA [diastolic suction (DS)]. The effect of the windkessel correction (i.e., using dP_{ex}, rather than dP_{meas}) is greatest during the acceleration phase of the E wave; quantitative results are presented in Table 3. The average energy of diastolic suction ($I_{W\text{-}DS}$) was 0.26 J/m^2 originally and increased by a factor of 2.6 (to 0.68 J/m^2) after the correction was applied. A *t*-test showed these values to be significantly different from zero, with $P = 0.0014$ and 0.0070, respectively. The paired *t*-test showed a significant effect of the correction ($P = 0.017$). $I_{W\text{-}DS}$ increased with LVEDP before and after the correction (Fig. 4). The relative increase was independent of LVEDP.

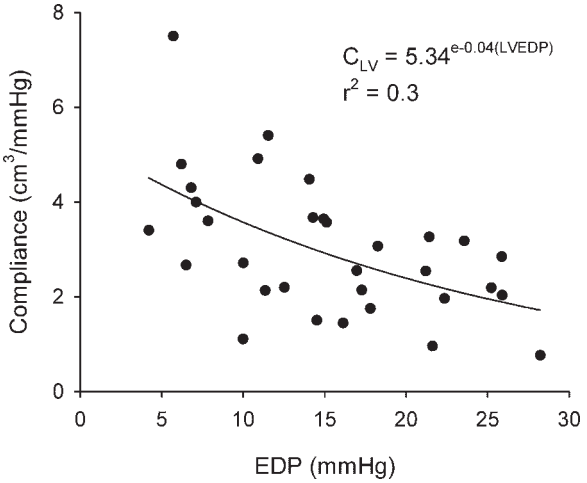

Fig. 3. C_{LV} plotted for all experiments vs. LV end-diastolic pressure (LVEDP). $P < 0.01$.

Table 2. *Exponential decay regression analysis results of C_{LV}*

Expt	C_{LV}	R^2
A	$5.24e^{-0.02(LVEDP)}$	0.27
B	$5.52e^{-0.04(LVEDP)}$	0.67
C	$4.91e^{-0.04(LVEDP)}$	0.59
D	$1.96e^{-5E-11(LVEDP)}$	0.00
E	$4.54e^{-0.07(LVEDP)}$	0.99
F	$9.68e^{-0.05(LVEDP)}$	0.89
All	$5.34e^{-0.04(LVEDP)}$	0.30

Results are from individual experiments as well as the cumulative plot in Fig. 3. C_{LV}, LV compliance.

Transmitral Flow vs. Velocity

Having scaled the rate of change of LV emptying (i.e., dV_{LV}/dt) to the integral of Q_{ao}, we can compare dV_{LV}/dt (equivalent to transmitral flow) with U_{mitral}. Averaged E wave patterns of dV_{LV}/dt and U_{mitral} from all experiments are shown in Fig. 5. The peak occurs substantially earlier for dV_{LV}/dt than for U_{mitral}. Peak dV_{LV}/dt occurs at approximately the time of the maximum left atrial pressure (P_{LA})-P_{LV} gradient; peak U_{mitral} occurs at approximately the time of the P_{LA}-P_{LV} crossover, i.e., when $P_{LA} = P_{LV}$.

Table 3. *$I_{W\text{-}DS}$ before and after windkessel correction*

Expt	$I_{W\text{-}DS}$, J/m^2	$I_{W\text{-}DS(corrected)}$, J/m^2	$I_{W\text{-}DS(corrected)}/I_{W\text{-}DS}$
A	0.18 (0.05)	0.40 (0.11)	2.23 (0.39)
B	0.18 (0.01)	0.50 (0.11)	2.91 (1.01)
C	0.36 (0.05)	1.13 (0.18)	3.27 (0.59)
D	0.17 (0.01)	0.40 (0.20)	2.31 (0.89)
E	0.40 (0.05)	1.20 (0.59)	2.97 (1.24)
F	0.29 (0.02)	0.45 (0.13)	1.61 (0.17)
Mean	0.26 (0.10)	0.68 (0.38)	2.6 (0.61)

Values are means (SD). $I_{W\text{-}DS}$, energy of diastolic suction.

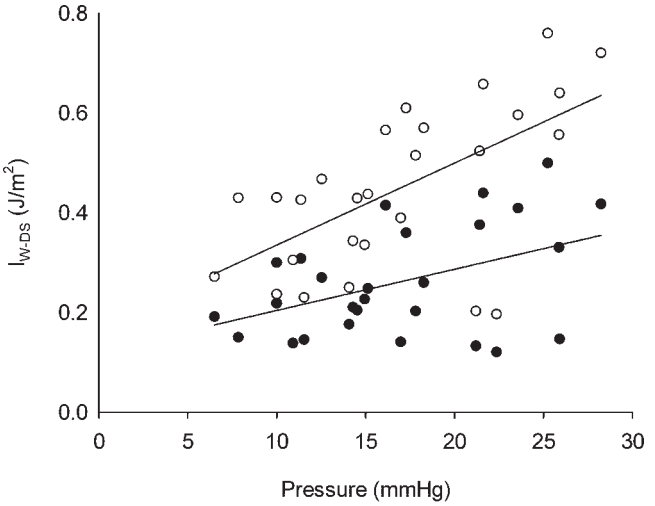

Fig. 4. Energy of early diastolic backward-going wave ($I_{W\text{-}DS}$) vs. LVEDP. ●, $I_{W\text{-}DS}$ from original WIA; ○, $I_{W\text{-}DS}$ from corrected WIA. $I_{W\text{-}DS}$ increases with volume loading. Original and corrected $I_{W\text{-}DS}$ are linearly correlated with increasing LVEDP (r^2 = 0.20 and 0.37, respectively).

DISCUSSION

Windkessel Correction

The parameters of WIA are calculated from incremental changes in pressure and velocity at a specific cross section of a vessel or chamber. Although the passage of waves clearly induces incremental changes in pressure, not all incremental changes in pressure are due to the passage of waves: changes in pressure may also be due to the elastance of a structure. For example, during isovolumic contraction and relaxation, ventricular pressure changes, because the elastance of the ventricle increases or decreases, respectively, while volume nominally remains constant. During these intervals, waves are absent. In contrast, when the LV ejects blood into the elastic (compliant) aorta, arterial pressure increases, because aortic inflow is temporarily greater than aortic outflow, and, thus, aortic volume increases (21). Therefore, to quantify properly the effects of waves on arterial pressure and velocity (flow), measured arterial pressure first must be "corrected" to exclude the component of the incremental change in pressure that is due only to this increase in arterial volume and not, fundamentally, due to the passage of waves. This is the rationale for separation of arterial pressure into the sum of a P_{Wk} and a wave-related pressure.

Windkessel Correction Applied to LV Filling

In this study, we have applied that same rationale to transmitral flow and found that the energy associated with DS was more than doubled (by a factor of 2.6) by the correction. This was because the corrected change in wave-related pressure (i.e., ΔP_{ex}) was greater than the change in P_{meas} (ΔP_{meas}) during early filling. Increasing volume is associated with increasing P_{Wk} because of the elastance of the passive LV. As illustrated in Fig. 1, P_{meas} decreased, despite the increasing volume, thus intimating that had it not been for the windkessel effect, the decrease in pressure would have been even greater than that actually measured.

Mitral Flow, Velocity, and Effective Area

This study extends and enhances our recent description of DS in the LV (23), in that we have shown that the magnitude of the energy we associate with DS is even greater after we account for the windkessel effect. However, the results of this study also raise new questions about our previous interpretations. We suggested previously that the energy of the BEW accelerated the motion of blood from the LA to the LV at the beginning of filling. This interpretation was consistent with the facts that the maximum P_{LA}-P_{LV} gradient coincided with the maximum rate of change of E wave velocity and that the peak E wave velocity was achieved when the P_{LA}-P_{LV} gradient returned to zero. [This timing is also supported by the work of Courtois et al. (3).] This relation of pressure gradient to

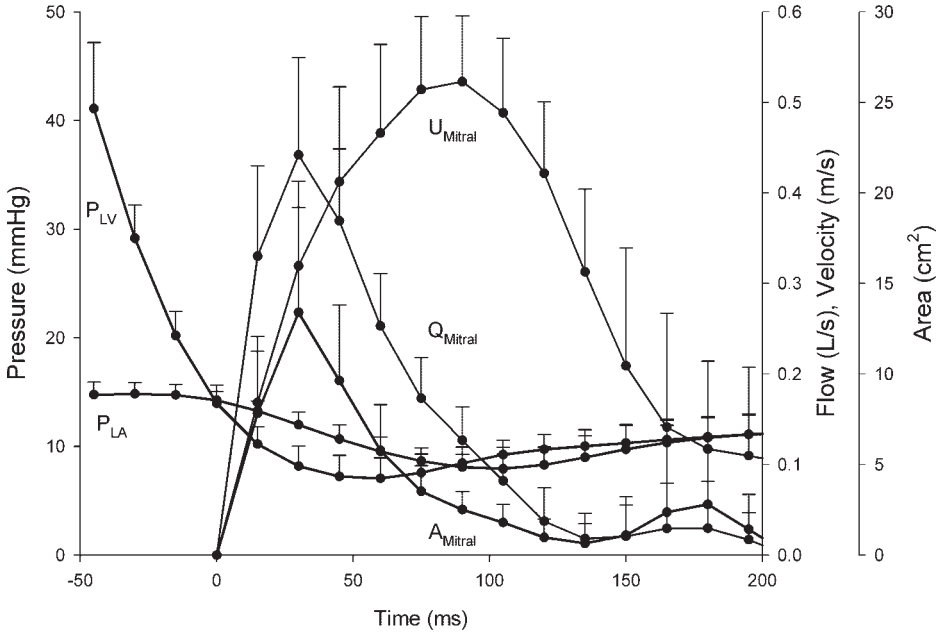

Fig. 5. Averaged filling parameters during early diastole (LVEDP ~14 mmHg). Mitral area (A_{mitral}) was calculated as change in V_{LV} with time (dV_{LV}/dt) divided by mitral velocity (U_{mitral}). Q_{mitral}, mitral flow.

velocity suggests that the inertia of the blood is important and dominant. As others had done before us (13), we implicitly assumed that the Doppler-measured flow velocity was representative of transmitral flow.

We found that the time course of LV filling during the E wave was markedly and fundamentally different, depending on whether it was assessed by velocity or volumetric flow (using the derivative of V_{LV} measured by sonomicrometry). As illustrated in Fig. 5, peak flow occurred relatively early, at the time of the peak P_{LA}-P_{LV} gradient. If both observations are to be accepted, it could be due to a decrease in effective mitral valve area, which would account for a high velocity, despite decreasing flow (9, 11). A similar conclusion was reached recently by Bowman et al. (2), who measured velocity by Doppler echocardiography and flow as the derivative of MRI-calculated V_{LV} in patients. However, our observation and that of Bowman et al. could be due to the vagaries of so-called shape changes. We found that V_{LV}, as estimated from orthogonal crystals, increased during "isovolumic" relaxation, producing nonrectangular P-V loops and $dV_{LV}/dt > 0$ (Fig. 6). These shape changes equate to a filling volume flow rate on the order of 50 ml/s, which is not insignificant on the scale of transmitral flow. An increase in V_{LV} during the isovolumic period has also been noted by others (1, 11, 16) and documented as an outward motion of the LV wall. Ruttley et al. (16) found that V_{LV} can increase up to 10% during this interval. If isovolumic relaxation is truly isovolumic, an outward motion must occur concurrently with an inward motion. Ruttley et al. and Altieri (1) pointed out that this change in LV shape may be fundamentally related to the descent of the mitral valve late in the isovolumic period. More recently, the work of Karlsson et al. (8) supported this view by demonstrating downward mitral leaflet motion before leaflet separation. The P-V loops published by Little et al. (11) appear to have the same nonrectangular shape as our P-V loop, indicating a volume change during isovolumic relaxation, but this does not appear to be consistent with their dV/dt plots. They suggest that the time course of LV dV/dt is similar to that of Doppler-measured U_{mitral}.

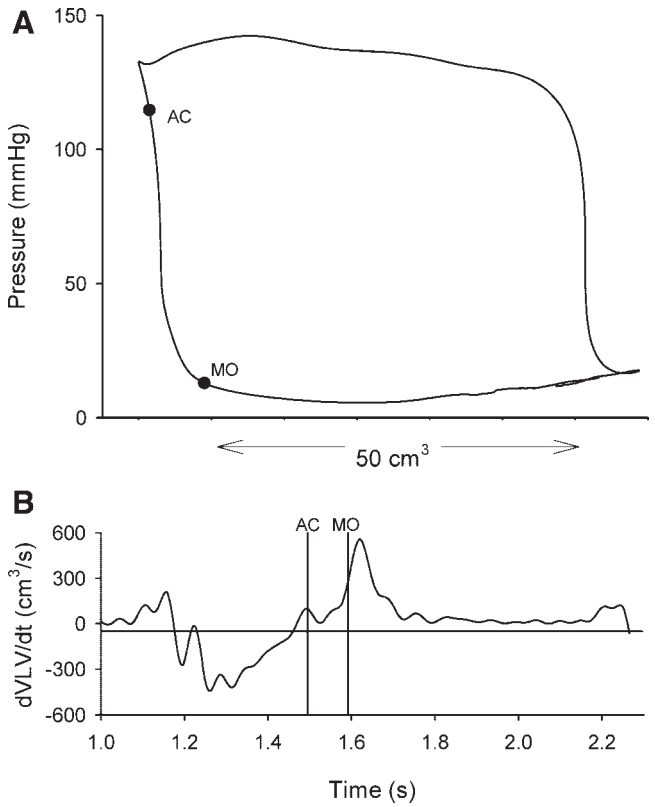

Fig. 6. *A*: LV pressure-volume (P-V) loop. *B*: time plot of dV_{LV}/dt. AC, aortic valve closure (AC); MO, mitral valve opening. Sloping P-V loop during isovolumic relaxation corresponds to increase in dV/dt before opening of mitral valve.

Since dV_{LV}/dt was positive before the P_{LA}-P_{LV} crossover in the present study, the dV_{LV}/dt values immediately after the crossover could not be ascertained reliably. If $dV_{LV}/dt > 0$ before the valve opens, it is inevitable that dV_{LV}/dt (i.e., flow) will be overestimated by an indeterminate amount immediately after the valve opens. An overestimation probably does occur, in that we and Bowman et al. (2) calculate effective mitral areas at the onset of the E wave that are too large and inconsistent anatomically (Fig. 5). Figure 5 displays our calculated effective mitral orifice area computed as the calculated flow divided by measured velocity. Further investigation is needed to resolve this calculated flow-velocity discrepancy and explain the effects of LV shape changes.

Limitations

These studies were conducted in open-chest anesthetized dogs, because it was not feasible to measure all these parameters in a more intact experimental preparation. Accordingly, artifacts may have been introduced, and the salient conclusions from this study require validation from more physiological experimental models or clinical observations.

Doppler echocardiography may underestimate true peak flow velocity for two reasons: *1*) placement of the sample volume is static, whereas the mitral annulus moves throughout diastole, displacing the leaflets and, therefore, the maximum-velocity location, and *2*) for measurement of the maximum velocity, the scan line must be exactly aligned with the flow, and any misalignment will underestimate the true velocity, in proportion to the cosine of the angle. Thus it is likely that the maximum-velocity point might be missed and/or it might be interrogated from a nonoptimal angle, especially if we consider that the view is only two-dimensional during recording.

As a first approximation and because of the limitations of the data, we used a linear estimate of C_{LV} as the basis for our windkessel correction. This approach neglects the effects of any possible changes in LA volume (V_{LA}) and the complexities of the LV P-V relation, which has been shown to be sigmoidal (12, 19). Thus, depending on the volume and the position along this sigmoidal relation, the correction for compliance could be even greater than we have shown. However, our intent was merely to illustrate the compliance dependence qualitatively. In principle, this study could be repeated with alternative techniques (e.g., MRI) that could account for V_{LA} and V_{LV} changes accurately.

In conclusion, the left heart reservoir function implies that changes in V_{LA} and V_{LV} will change pressure, and when these changes in pressure are discounted, we find that the energy associated with DS is more than twice as great as that calculated previously. In principle, within the heart as well as in the

vasculature, volume-related changes in pressure (i.e., the windkessel or reservoir effect) should be discounted when the effects of wave motion are assessed.

APPENDIX

WIA. The energy associated with waves traveling throughout the cardiovascular system can be quantified using WIA. Net intensity (dI_W) is the product of the incremental pressure (dP) and incremental velocity (dU), both measured at the same location. Intensity is a power flux and can be expressed in W/m^2. If we know the density (ρ) of the blood and the wave speed (c), intensities of simultaneous forward- and backward-going waves (dI_{W+} and dI_{W-}, respectively) can be calculated separately (14, 18)

$$dI_{W+} = \left(+ \frac{1}{4}\rho c \right)(dP + \rho c dU)^2 \quad (A1)$$

$$dI_{W-} = \left(- \frac{1}{4}\rho c \right)(dP - \rho c dU)^2 \quad (A2)$$

Intensities of forward-going (i.e., in the direction of net blood flow) waves are conventionally denoted as positive and backward-going waves as negative. The net energy of a wave is calculated as the time integral of the net intensity (14, 18).

The characteristics of a wave (i.e., expansion or compression) are distinguished by the sign of dP

$$dP_+ = \frac{1}{2}(dP + \rho c dU) \quad (A3)$$

$$dP_- = \frac{1}{2}(dP - \rho c dU) \quad (A4)$$

where dP_+ and dP_- correspond to the incremental change in pressure caused by a wave. Positive values indicate compression waves, and negative values indicate expansion waves.

ACKNOWLEDGMENTS

We thank Dr. Richard Thompson for contributions and helpful insight on mitral valve dynamics, Cheryl Meek for outstanding surgical skills, and Rozsa Sas for help with figure preparation.

REFERENCES

1. **Altieri PI.** Left ventricular wall motion during the isovolumic relaxation period. *Circulation* 48: 499–505, 1973.
2. **Bowman AW, Frihauf PA, Kovacs SJ.** Time-varying effective mitral valve area: prediction and validation using cardiac MRI and Doppler echocardiography in normal subjects. *Am J Physiol Heart Circ Physiol* 287: H1650–H1657, 2004.
3. **Courtois M, Kovacs SJ Jr, Ludbrook PA.** Transmitral pressure-flow velocity relation: importance of regional pressure gradients in the left ventricle during diastole. *Circulation* 78: 661–671, 1988.
4. **Frank O.** Die Grundform des Arteriellen Pulses. *Erste Abhandlung Mathematische Analyse Z Biol* 37: 483–526, 1899.
5. **Gaynor JW, Feneley MP, Gall SA Jr, Maier GW, Kisslo JA, Davis JW, Rankin JS, Glower DD Jr.** Measurement of left ventricular volume in normal and volume-overloaded canine hearts. *Am J Physiol Heart Circ Physiol* 266: H329–H340, 1994.
6. **Grant C, Bunnell IL, Greene DG.** The reservoir function of the left atrium during ventricular systole. An angiocardiographic study of atrial stroke volume and work. *Am J Med* 37: 36–43, 1965.
7. **Johnston WE, Vinten-Johansen J, Tommasi E, Little WC.** ULFS-49 causes bradycardia without decreasing right ventricular systolic and diastolic performance. *J Cardiovasc Pharmacol* 18: 528–534, 1991.
8. **Karlsson MO, Glasson JR, Bolger AF, Daughters GT, Komeda M, Foppiano LE, Miller DC, Ingels NB Jr.** Mitral valve opening in the ovine heart. *Am J Physiol Heart Circ Physiol* 274: H552–H563, 1998.
9. **Lee CS.** *Fluid Mechanical Studies of Mitral Valve Motion* (Ph.D. thesis). Berkeley: University of California, 1977.
10. **Lighthill MJ.** *Waves in Fluids*. Cambridge, UK: Cambridge University Press, 1978, p. 106.
11. **Little WC, Ohno M, Kitzman DW, Thomas JD, Cheng CP.** Determination of left ventricular chamber stiffness from the time for deceleration of early left ventricular filling. *Circulation* 92: 1933–1939, 1995.
12. **Nikolic S, Yellin EL, Tamura K, Vetter H, Tamura T, Meisner JS, Frater RWM.** Passive properties of canine left ventricle: diastolic stiffness and restoring forces. *Circ Res* 62: 1210–1222, 1988.
13. **Otto CM.** Echocardiographic evaluation of ventricular diastolic filling and function. In: *Textbook of Clinical Echocardiography*. Philadelphia, PA: Saunders, 2003, p. 132–152.
14. **Parker KH, Jones CJH.** Forward and backward running waves in the arteries: analysis using the method of characteristics. *J Biomech Eng* 112: 322–326, 1990.
15. **Rankin JS, McHale PA, Arentzen CE, Ling D, Greenfield JC, Anderson RW.** The three-dimensional dynamic geometry of the left ventricle in the conscious dog. *Circ Res* 39: 304–313, 1976.
16. **Ruttley MS, Adams DF, Cohn PF, Abrams HL.** Shape and volume changes during "isovolumetric relaxation" in normal and asynergic ventricles. *Circulation* 50: 306–316, 1974.
17. **Scott-Douglas NW, Traboulsi M, Smith ER, Tyberg JV.** Experimental instrumentation and left ventricular pressure-strain relationship. *Am J Physiol Heart Circ Physiol* 261: H1693–H1697, 1991.
18. **Sun YH, Anderson TJ, Parker KH, Tyberg JV.** Wave-intensity analysis: a new approach to coronary dynamics. *J Appl Physiol* 89: 1636–1644, 2000.
19. **Tyberg JV, Keon WJ, Sonnenblick EH, Urschel CW.** Mechanics of ventricular diastole. *Cardiovasc Res* 4: 423–428, 1970.
20. **Wang JJ, Flewitt JA, Shrive NG, Parker KH, Tyberg JV.** Systemic venous circulation. Waves propagating on a windkessel: relation of arterial and venous windkessels to systemic vascular resistance. *Am J Physiol Heart Circ Physiol* 290: H154–H162, 2006.
21. **Wang JJ, O'Brien AB, Shrive NG, Parker KH, Tyberg JV.** Time-domain representation of ventricular-arterial coupling as a windkessel and wave system. *Am J Physiol Heart Circ Physiol* 284: H1358–H1368, 2003.
22. **Wang JJ, Parker KH, Tyberg JV.** Left ventricular wave speed. *J Appl Physiol* 91: 2531–2536, 2001.
23. **Wang Z, Jalali F, Sun YH, Wang JJ, Parker KH, Tyberg JV.** Assessment of left ventricular diastolic suction in dogs using wave-intensity analysis. *Am J Physiol Heart Circ Physiol* 288: H1641–H1651, 2005.